

Learning Curve Associated with ClearPoint Neuronavigation System: A Case Series

Birra R. Taha¹, Christian R. Osswald⁴, Matthew Rabon⁴, Carolina Sandoval Garcia¹, Daniel J. Guillaume¹, Xiao Wong², Andrew S. Venteicher¹, David P. Darrow¹, Michael C. Park^{1,3}, Robert A. McGovern¹, Cornelius H. Lam¹, Clark C. Chen¹

■ **BACKGROUND:** The ClearPoint neuronavigation system affords real-time magnetic resonance imaging (MRI) guidance during stereotactic procedures. While such information confers potential clinical benefits, additional operative time may be needed.

■ **METHODS:** We conducted a retrospective analysis of procedural time associated with ClearPoint Stereotaxis, with hypothesis that this procedural time is comparable with that associated with frame-based biopsies.

■ **RESULTS:** Of the 52 patients evaluated, the total procedural time for ClearPoint stereotactic biopsy averaged 150.0 (± 40.4) minutes, of which 111.5 (± 16.5) minutes were dedicated to real-time MRI acquisition and trajectory adjustment. This procedural time is within the range of those reported for frame-based needle biopsies. Approximately 5 minutes of the procedural time is related to the mounting of the MRI-compatible stereotactic frame. Based on the procedural time, we estimate that four cases are required in the learning curve to achieve this efficiency. Efficient algorithms for distortion corrections and isocenter localization are keys to ClearPoint stereotaxis. Routine quality assurance/control after each MRI software update and institutional information technology maintenance also contribute to efficiency. Real-time MRI is essential for definitive diagnosis in select cases.

■ **CONCLUSIONS:** ClearPoint stereotactic needle biopsy can be achieved in time frames comparable to frame-based stereotaxis. However, procedural efficiency requires 4

“learning curve” cases as well as vigilance in terms of MR distortion correction and information technology maintenance.

INTRODUCTION

Technology adoption in neurosurgery is a complex process that involves considerations beyond procedural improvements conferred and patient benefits actualized.¹ The resource demands,² steepness of the learning curve,³ and compatibility with existing technology platforms³ are key elements that influence technology adoption. Here, we examine the learning curve for the ClearPoint navigation as a platform for stereotaxis in the setting of needle biopsy and/or laser ablation therapy. Specifically, we conducted a retrospective analysis of procedural time associated with ClearPoint stereotaxis to determine the required learning curve. We further compared ClearPoint procedural time with that associated with frame-based biopsy.

The ClearPoint platform consists of an integrated hardware and software system that provides real-time magnetic resonance imaging (MRI) guidance during the procedure (Figure 1). In neuro-oncology, the platform has been adopted for the biopsy of technically challenging lesions, including subcubic centimeter lesions,⁴ lesions located in the deep gray matter/brainstem,^{4,5} and lesions adjacent to critical anatomy, such as the sellar/periventricular region.^{6,7} Relative to conventional stereotactic needle biopsies, where the biopsy trajectory is determined based on preoperative imaging, the ClearPoint platform allows real-time trajectory visualization and adjustment during the

Key words

- ClearPoint
- IMRIS
- Intracranial biopsy
- Intracranial laser ablation
- Neurosurgery
- Targeted drug delivery

Abbreviations and Acronyms

- LITT:** Laser interstitial thermal therapy
MRI: Magnetic resonance imaging

From the Departments of ¹Neurosurgery, ²Radiology, and ³Neurology, University of Minnesota Medical School, Minneapolis, Minnesota; and ⁴ClearPoint Neuro, Inc., Irvine, California, USA

To whom correspondence should be addressed: Clark C. Chen, M.D., Ph.D.
[E-mail: ccchen@umn.edu]

Citation: *World Neurosurg.* X (2022) 13:100115.
<https://doi.org/10.1016/j.wnsx.2021.100115>

Journal homepage: www.journals.elsevier.com/world-neurosurgery-x

Available online: www.sciencedirect.com

2590-1397/© 2021 The Author(s). Published by Elsevier Inc. This is an open access article under the CC BY-NC-ND license (<http://creativecommons.org/licenses/by-nc-nd/4.0/>).

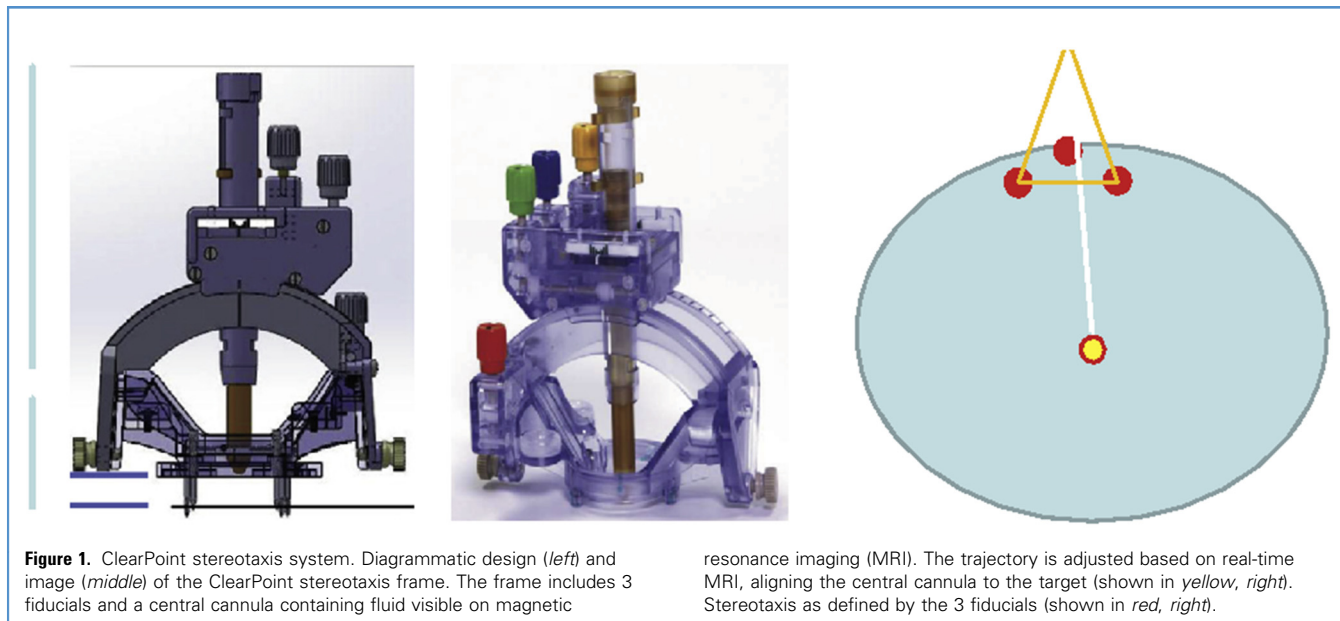


Figure 1. ClearPoint stereotaxis system. Diagrammatic design (*left*) and image (*middle*) of the ClearPoint stereotaxis frame. The frame includes 3 fiducials and a central cannula containing fluid visible on magnetic

resonance imaging (MRI). The trajectory is adjusted based on real-time MRI, aligning the central cannula to the target (shown in *yellow*, *right*). Stereotaxis as defined by the 3 fiducials (shown in *red*, *right*).

procedure.⁴⁻⁷ This adjustment enhances the accuracy of stereotaxis by allowing opportunities to correct for unintended technical mishaps, such as deviation from the intended Burr hole during drilling (“skiving”),⁷ and accommodates anatomic shifts resulting from cerebrospinal fluid egress.⁸ Moreover, the platform is compatible with laser interstitial thermal therapy (LITT), also known as stereotactic laser ablation,^{9,10} which can be performed immediately after the biopsy or as an independent procedure.^{11,12} In addition, the ClearPoint platform is compatible with the delivery of biological therapies.¹³

ClearPoint-aided procedures can be broadly divided into 2 stages: 1) mounting of the MRI-compatible stereotactic frame with optimization of stereotactic trajectory based on real-time MRI, and 2) performing the intended procedure (e.g., needle biopsy, laser ablation). The procedural elements in the second half of the ClearPoint procedure are comparable with those done without ClearPoint. We, therefore, studied the resource demands unique to ClearPoint stereotaxis by characterizing the associated operative time (henceforth referred as ClearPoint stereotaxis time). We further studied this time as the procedure was performed in different MR systems, including a diagnostic GE Discovery 3.0T, a Philips Intera 1.5T intraoperative MRI (1.5T), and an IMRIS Siemens Skyra 3.0T intra-operative MRI (3T). The learning curve during these transitions were characterized and key lessons shared. Information provided in this study should inform the decision of whether an institution should adopt this technology and mitigate adoption-associated challenges.

METHODS

Patient Population and Data Collection

ClearPoint stereotaxis was used to aid stereotactic needle biopsies, laser thermal ablations, or administration of therapeutic agents in patients undergoing clinical trial testing. Criteria for ClearPoint

stereotaxis included subcentimeter contrast-enhancing lesions,⁴ lesions located in the deep gray matter/brain stem,^{6,7} and lesions adjacent to critical anatomical structures such as the sellar⁷ or periventricular regions.⁶ Procedures were performed from 2015 to 2020 using 3 distinct MRIs: GE Discovery 3.0T MR 750w, Philips Intera 1.5T dedicated intraoperative MRI, and a Siemens Skyra 3.0T intraoperative MRI. Corresponding clinical information from each procedure was collected under protocols, with patient consent waived, as approved by the institutional review board. All procedures were performed by the senior author (C.C.C.).

Description of ClearPoint Stereotaxis Time

All procedures were performed with the patient under general anesthesia. As previously described,¹¹ the trajectory was adjusted based on MRI scans acquired in real-time after mounting of an MRI-compatible stereotactic frame. The ClearPoint multipositional head fixation frame (ClearPoint Neuro, Irvine, California, USA) was used for head immobilization in the Phillips procedures and the HFD100 Head Fixation Device (IMRIS and Deerfield Imaging, Inc., Minnetonka, Minnesota, USA) was used for the Skyra procedures. The time elapsed between the pinning and the final target confirmation was defined as ClearPoint stereotaxis time. For each procedure, the radial error was calculated (defined as the distance from the intersection of the device trajectory with the planned target axis). In all biopsies, the procedure was not terminated until pathologic tissue is confirmed on frozen pathology.

Statistical Analysis

Average ClearPoint stereotaxis time and procedural times were analyzed. Comparison in time required for ClearPoint stereotaxis was done using the Student t test. R, version 3.3.2 (R Foundation

Table 1. Lesion Characteristics, ClearPoint Stereotaxis Time, and Total Procedural Time

Site/MRI	Laterality	Location	Max Diameter (CE)*	Cancer Type	Procedure	Stereotaxis Time	Procedural Time†
UCSD/GE							
1	L	Thalamus	19	Colon cancer, recurrent	Biopsy + LITT	210	260
2	L	Corpus callosum (genu)	18	IDHwt GBM, recurrent	LITT	150	240
3	R	Frontal	23	IDHwt GBM	LITT	180	235
4	R	Temporal	8	IDHwt GBM, recurrent	Biopsy + LITT	195	300
5	R	Frontal	18	IDHwt GBM	LITT	130	175
6	R	Basal ganglia (caudate)	10	Breast cancer, recurrent	Biopsy + LITT	90	180
7	L	Periventricular	10	IDHwt GBM	Biopsy	105	195
8	L	Mesial temporal	9	IDHwt GBM	Biopsy	90	155
9	B	Corpus callosum (splenium)	16	IDHwt GBM, recurrent	LITT	120	305
10	L	Temporal-parietal	8	IDHwt GBM, recurrent	Biopsy + LITT	130	291
11	L	Periventricular	7	Lymphoma	Biopsy	130	249
12	L	Thalamus	13	IDHwt GBM, recurrent	Biopsy + LITT	115	148
13	L	Middle cerebellar peduncle	8	H3K27M glioma	Biopsy + LITT	90	195
14	R	Peritrial	6	Lymphoma	Biopsy	125	145
		Average	13.25			132.86 ± 38.4	219.50 ± 56.6
UMMC/Philips							
1	L	Periventricular	27	IDHm, anaplastic astrocytoma	Biopsy + LITT	108	259
2	B	Corpus callosum (genu)	22	IDHwt GBM, recurrent	LITT	117	210
3	Midline	Pineal gland	24	Pineocytoma	LITT	135	273
4	Midline	Corpus callosum (splenium)	28	IDHwt GBM, Recurrent	LITT	145	278
5	R	Basal ganglia (caudate)	31	Lymphoma	Biopsy	108	255
6	R	Occipital	6	Cavernous malformation	LITT	135	199
7	L	Cerebellar	14	Metastasis, recurrent	Biopsy + LITT	135	298
8	L	Thalamus	29	H3K27M Glioma, recurrent	Biopsy‡	80	212
9	R	Insular	28	IDHwt GBM, recurrent	LITT	112	183
10	L	Thalamus	11	H3K27M glioma, recurrent	Biopsy†	93	105
11	L	Thalamus	14	H3K27M glioma, recurrent	Biopsy†	110	134
12	R	Periventricular	24	IDHwt GBM, recurrent	Biopsy	102	107
13	R	Third ventricle	23	H3K27M glioma, recurrent	Biopsy†	89	131
14	R	Basal ganglia (caudate)	26	IDHwt GBM, recurrent	Biopsy	117	127
		Average	21.93			113.29 ± 18.4	197.93 ± 65.5
UMMC/IMRIS							
1	R	Frontal	10	IDHwt GBM	Biopsy	245	282
2	L	Temporal	14	Metastasis, recurrent	Biopsy + LITT	124	269

Shown are the characteristics of lesions treated, including maximal diameter, indication, tissue diagnosis, operative time, and procedural time.

MRI, magnetic resonance imaging; UCSD, University of California San Diego; L, left; LITT, laser interstitial thermal therapy; IDHwt, wild-type isocitrate dehydrogenase; GBM, glioblastoma; R, right; UMMC, University of Minnesota Medical School.

*Max diameter (CE): maximal diameter of the contrast-enhancing region.

†Procedural time include time to frozen diagnosis confirming diagnostic tissue.

‡Clinical trial case, time estimate does not include oncolytic virus infusion.

Continues

Table 1. Continued

Site/MRI	Laterality	Location	Max Diameter (CE)*	Cancer Type	Procedure	Stereotaxis Time	Procedural Time†
3	L	Medulla	7	IDHwt GBM	Biopsy	138	168
4	R	Periventricular	28	Lymphoma	Biopsy	116	146
5	R	Basal Ganglia	23	IDHwt GBM, recurrent	Biopsy + LITT	135	140
6	R	Periventricular	9	Radiation necrosis	Biopsy	220	265
7	R	Temporal	42	Meningioma	LITT	106	161
8	R	Frontal	15	IDHwt, GBM	LITT	157	240
9	R	Thalamus	10	Gliosis	Biopsy	105	275
10	R	Thalamus	21	H3K27M Glioma	Biopsy	106	195
11	R	Thalamus	17	Infiltration glioma	Biopsy	117	183
12	R	Periventricular	22	Radiation necrosis	Biopsy + LITT	147	249
13	R	Periventricular	29	Metastasis, recurrent	Biopsy + LITT	105	127
14	L	Periventricular	9	IDHwt GBM, recurrent	Biopsy + LITT	117	182
		Average	18.29			138.43 ± 41.8	205.86 ± 53.4

Shown are the characteristics of lesions treated, including maximal diameter, indication, tissue diagnosis, operative time, and procedural time.
 MRI, magnetic resonance imaging; UCSD, University of California San Diego; L, left; LITT, laser interstitial thermal therapy; IDHwt, wild-type isocitrate dehydrogenase; GBM, glioblastoma; R, right; UMMC, University of Minnesota Medical School.
 *Max diameter (CE): maximal diameter of the contrast-enhancing region.
 †Procedural time include time to frozen diagnosis confirming diagnostic tissue.
 ‡Clinical trial case, time estimate does not include oncolytic virus infusion.

for Statistical Computing, Vienna, Austria) was used for statistical analysis.¹⁴

RESULTS

Study Cohort

The locations, maximal diameter of contrast enhancement in the lesion treated, the indications, tissue diagnosis, operative time, and procedural time are shown in **Table 1**. The first ClearPoint procedures were performed in the GE Discovery 3.0T MR 750w (70 cm bore). While several were performed in this case series (biopsy, laser ablation and administration of DNATrix 2401, an oncolytic virus^{13,15}) the procedural elements involving ClearPoint stereotaxis were fundamentally the same. Calculated target radial errors for all procedures performed were <2 mm. All biopsies performed yielded diagnostic tissues. There was no procedural morbidity or mortality. Except for 2 DNATrix-treated subjects, all patients who underwent ClearPoint procedures were discharged home on postoperative day 1 without complications or readmission. One DNATrix 2401-infused patient was discharged to rehabilitation on postoperative day 5 due to pre-existing neurologic deficits. The second patient was discharged home on postoperative day 1 but readmitted on postoperative day 3 for an incapacitating headache that resolved with steroid treatment.

Operative Time Associated with ClearPoint Stereotaxis

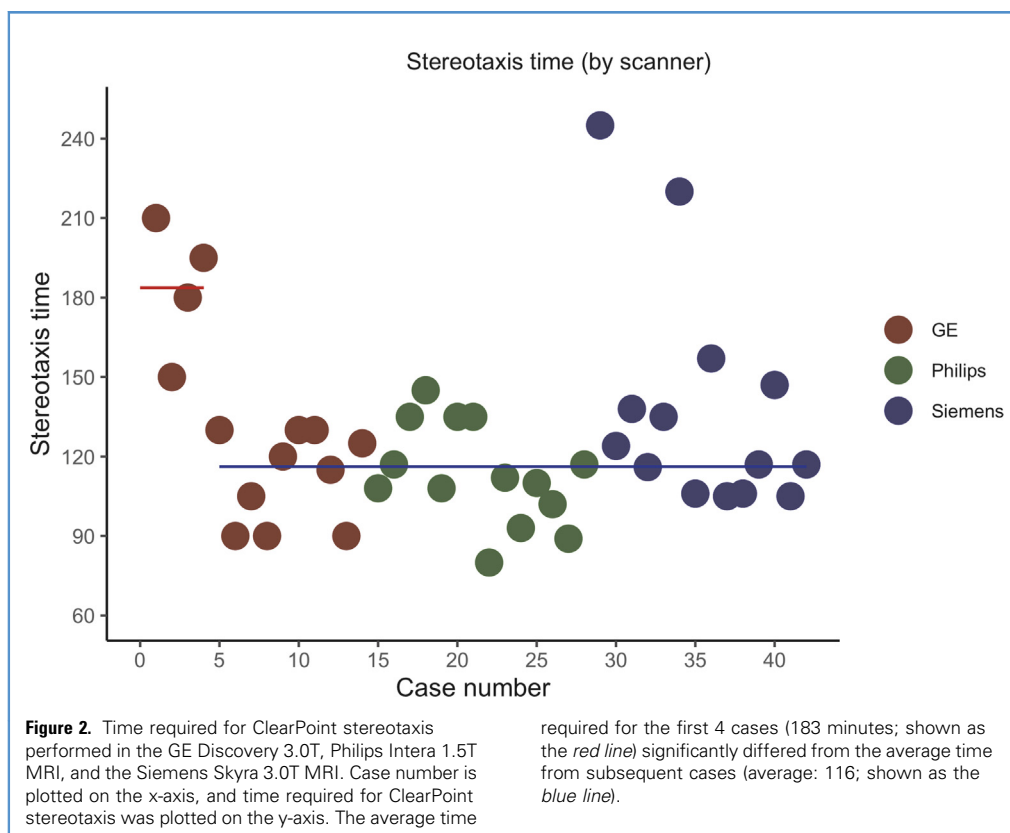
While real-time adjustments in stereotactic trajectories confer potential procedural benefits,¹⁶ the process may be associated

with increased operative time. Since operating room availability is a rate-limiting resource for the adoption of surgical innovations,¹⁷ we quantified the operative time associated with the ClearPoint stereotaxis, defined as the time between completion of head pinning and completion of trajectory adjustment.

Figure 2 shows the time required for ClearPoint stereotaxis for the first 14 cases for each of the 3 scanners. After the first 4 cases in the GE scanner, the ClearPoint stereotaxis time consistently ranged between 90 and 120 minutes (mean of 116.2 minutes), with rare exceptions, which are discussed to follow.

Despite a difference in bore size between the Phillips suite (60 cm) and the GE scanner (70 cm), the time required for ClearPoint stereotaxis in the Phillips suite (113 ± 19 minutes) was comparable with those performed in the GE scanner, suggesting that lessons learned on the GE scanner were “transplantable” to another MR scanner (**Figure 2**).

The ClearPoint procedures were subsequently performed in a Siemens Skyra 3.0T. Like the GE Discovery scanner, the Skyra 3.0T hosts a 70-cm bore. The first procedure in the Skyra 3.0T required 245 minutes (**Figure 2**, asterisked case). The procedure was protracted because of image distortion secondary to suboptimal patient placement relative to the smaller isocenter of the Skyra 3.0T magnet relative to the Phillips 1.5T magnet (**Figure 3A–B**). This issue was ultimately addressed by 1) moving the patient to align isocenter to the mid-point of the ClearPoint stereotactic frame (**Figure 3C**) and 2) implementation of appropriate image distortion correction algorithms (**Figures 4A–B**). Specifically, the default protocol uses 2-dimensional distortion correction,



which failed to adequately correct image distortion. This issue was resolved by using a 3-dimensional distortion correction. After resolving issues related to image distortion and isocenter localization, the time required for ClearPoint stereotaxis again returned to 90–120 minutes (Figure 2). The one exception involved case 6 (Figure 2, double asterisk case) where routine information technology and scanner update issues led to challenges in information transfer between the scanner and the ClearPoint system. Ultimately, the images DICOM images were transferred through a USB drive.

Quantitative Analysis of Learning Curve for ClearPoint Stereotaxis

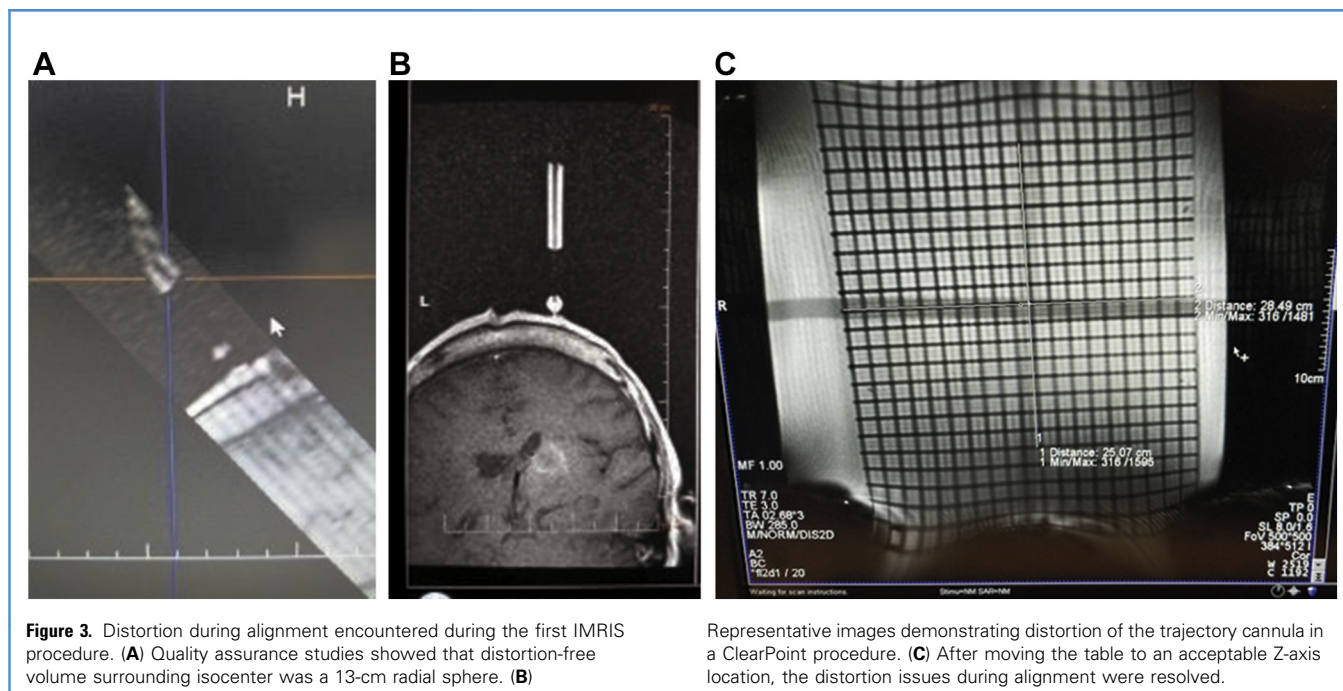
We wished to provide a rigorous determination of the number of cases required in this learning curve. To this end, we compared the mean ClearPoint stereotaxis time of the first 2, 3, 4, 5, and 6 cases relative to the next cohort of the same number of cases that immediately followed. For instance, we compared the ClearPoint stereotaxis time for cases 1-2 relative to 3-4, for cases 1-3 relative to 4-6, for cases 1-4 relative to 5-8, etc. As shown in Table 2, the minimal number of cases after which the mean ClearPoint stereotaxis time decreased significantly was 4. We next compared the running average of ClearPoint stereotaxis time for sequential 4 cases. For example, we compared the ClearPoint stereotaxis time for cases 1-4 relative to 5-8, for cases 2-5 relative to 6-9, for cases 3-6 relative to 7-10, etc. As shown in Table 3, the average ClearPoint stereotaxis time for the initial 4 cases remained significantly greater than the subsequent 4 cases until the cohort that started with case 4 (i.e., comparing cases 4-7

and cases 8-11). This finding again suggests that 4 cases are required for the learning curve. Finally, we compared the average ClearPoint stereotaxis time of the first 4 cases relative to a randomly selected 4 subsequent cases from any of the 3 MRI scanners (excluding the anomalous cases described previously and the initial 4 cases). We fitted a Gaussian distribution against ClearPoint stereotaxis time averages from all combinations ($n = 46,736$) and showed that the average ClearPoint stereotaxis time of the first 4 cases was significantly greater ($P < 0.001$, Supplementary Figure 1). In aggregate, these analyses provide an estimated number of 4 cases that define the learning curve.

Total Procedural Time

The average total procedure time (Table 1) for ClearPoint-aided needle biopsy was 150.0 ± 40.4 minutes, with 111.5 ± 16.5 minutes devoted to stereotactic alignment. The protracted cases involved cases requiring additional biopsy trajectory adjustment or confirmation of diagnostic tissues on frozen pathology. The total procedural time for ClearPoint aided stereotactic needle biopsy is within the range of published procedural times for frame-based stereotactic needle biopsies (ranged averages of 54–149 minutes).¹⁸

An average of 222.9 ± 63.0 minutes was required for completion of procedures combining LITT and biopsy. An average of 227.2 ± 46.1 minutes was required for LITT-only procedures. The addition of a biopsy to LITT did not significantly increase the total procedural time.



Frame Placement

A key procedural aspect of ClearPoint stereotaxis involves mounting of an MRI-compatible frame. We measured the time required for this procedural element as a function of the number of ClearPoint procedures performed to characterize the learning curve. The first frame mounted (Table 4) required approximately 12 minutes. After the first 4 procedures, the time required for frame mount stabilized to approximately 5 minutes.

Sequential Depth Biopsies

In cases in which nondiagnostic tissues were secured on the initial biopsy, the following maneuvers were performed. A repeat MRI is done to 1) confirm the location of the needle relative to the lesion and 2) assess potential biopsy site hematoma. If no hematoma is observed and the direction of the cutting window is suboptimal, the biopsy needle is rotated to align to the cutting window to the lesion. If the biopsy window is optimal, the biopsy needle is advanced by 2–5 mm and a biopsy is repeated. This maneuver is performed because we used axial MRI scans as the source of our stereotaxis. While this approach optimizes anatomic delineation in the axial, x-y plan, the rostral–caudal anatomy is extrapolated. We have found that such extrapolation can lead to overestimation of depth. A representative case in which sequential depth biopsy yielded diagnostic tissue while the initial biopsy did not is shown in Figure 5. Histologic characteristics of this representative case is shown in Figure 6.

DISCUSSION

Real-time visualization of the intracranial compartment during challenging stereotaxis allows opportunities for trajectory

adjustment to improve the accuracy and safety of the procedure.¹⁹ ClearPoint neuronavigation was developed with this central premise. However, this visualization and adjustment can come at the cost of an increased procedural time. In this retrospective analysis, we analysis of procedural time associated with ClearPoint Stereotaxis. We estimate that the learning curve of ClearPoint stereotaxis based on the number of procedures required for stabilization of procedural time. This analysis suggests that the learning curve for a surgeon naïve to this system is approximately 4 cases. After this learning curve, the added time associated with real-time visualization and trajectory adjustment became 111.5 ± 16.5 minutes. Accounting for the time required for completion of the actual biopsy and confirmation of pathologic tissue securement, the total procedural time for ClearPoint-aided stereotactic needle biopsy (150.0 ± 40.4 minutes) is within the range of those reported for frame-based needle biopsies (ranged averages of 54–149 minutes).^{20,21}

Our study suggests that technology demand and not procedural complexity constitutes the main driving force behind the protracted time for ClearPoint stereotaxis. The procedural element of the procedure involves the mounting of an MRI-compatible stereotactic frame, which is technically straightforward and can be achieved in approximately 5 minutes. Our study further suggests that most workflow efficiencies for ClearPoint stereotaxis are transplantable between different MRI systems. The technical demands of image distortion correction and isocenter identification, on the other hand, require customization to the particular institution's MRI system used to support ClearPoint stereotaxis. In addition, routine MRI software updates can disrupt communication between the MRI and the ClearPoint Neuro Navigation System. As such, routine quality assurance processes are

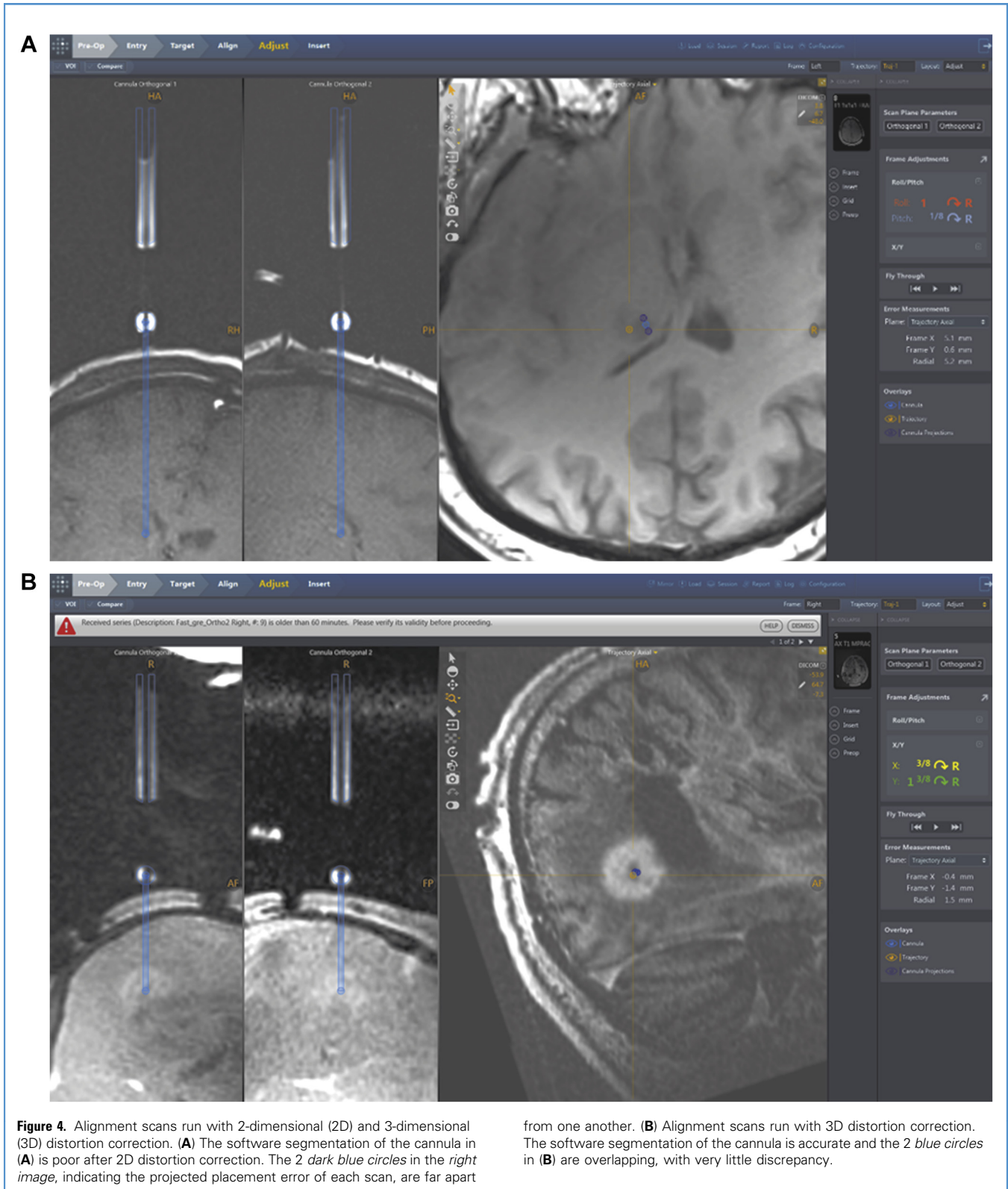


Table 2. Minimal Number of Cases After Which ClearPoint Stereotaxis Time Stabilized

Number of Cases	Average	Subsequent Case Average	P Value
2 cases	180.0	187.5	0.831
3 cases	180.0	138.3	0.302
4 cases	183.8	103.8	0.002
5 cases	173.0	107.0	0.004
6 cases	159.2	115.0	0.046

Mean ClearPoint stereotaxis time of the first 2, 3, 4, 5, and 6 cases was compared to the next cohort of the same number of cases that immediately followed. For instance, we compared the ClearPoint stereotaxis time for cases 1–2 relative to 3–4, for cases 1–3 relative to 4–6, for cases 1–4 relative to 5–8, etc.

warranted after each MR software update or institutional information technology audit. Maintaining a support team familiar with ClearPoint stereotaxis is equally important for an efficient workflow.

Interpretation of the total procedural time required for a stereotactic needle biopsy warrants further discussion. It is possible to achieve operative time efficiency of a needle biopsy by terminating the procedure before confirmation of diagnostic tissue on frozen pathology; and, such confirmation may not be necessary when a sizable lesion is biopsied. However, the cases that we have selected for ClearPoint stereotaxis were those considered challenging. Several of these cases were described in our previous publications.^{4–7} Given the challenging nature of these lesions, we felt that frozen pathology confirmation is warranted.

Our case series report consecutive cases without arbitrary patient exclusion. In total, we evaluated 52 patients who underwent ClearPoint stereotactic procedures over a span of 5 years. We found the procedural time for ClearPoint stereotaxis, after the initial learning curve, is remarkably constant despite the use of different intraoperative MRI suites. In general, we used ClearPoint for small lesions (typically <1 cm) located in the deep gray matter/brainstem or adjacent to critical anatomies (such as the middle

Table 3. Comparison of the Running Averages of ClearPoint Stereotaxis for Sequential Four Cases

Case Number	Average	Subsequent Four Average	P Value
Cases 1–4	183.8	103.8	0.002
Cases 2–5	163.75	111.25	0.009
Cases 3–6	148.75	103.75	0.022
Cases 4–7	130	117.5	0.535
Cases 5–8	103.75	123.75	0.096
Cases 6–9	101.25	116.25	0.253
Cases 7–10	111.25	115	0.077

We compared the ClearPoint stereotaxis time for cases 1–4 relative to 5–8, for cases 2–5 relative to 6–9, for cases 3–6 relative to 7–10, etc.

Table 4. Time Required for Mounting of ClearPoint Stereotaxis Frame

Procedures	Time (minutes.seconds)
1	12.35
2	8.43
3	5.25
4	6.34
5	4.5
6	5.3
7	4.37
8	5.57
9	5.45
10	4.42

The time required for mounting the magnetic resonance imaging-compatible ClearPoint frame was measured as a function of the number of procedures performed.

cerebral artery). Extrapolation of our dataset beyond this patient population warrants caution.

Another major limitation of this study relates to generalizability of this single institutional experience. In this context, it is reassuring that the results remained similar irrespective of the MR suite and comparable to quality assurance data that ClearPoint Neuro, Inc., has collected in other institutions.²² An added complexity to the information presented is that time required for ClearPoint stereotaxis can be shortened if ClearPoint is used in combination with frameless stereotaxy.²³ In contrast, procedures that require multiple trajectories¹¹ or the biopsy of challenging locations²⁴ may significantly increase the time required for ClearPoint stereotaxis. Despite these limitations, our study provides valuable, quantitative information that should aid in the decision of technology adoption and resource allocation as it relates to ClearPoint stereotaxis.

CONCLUSIONS

ClearPoint affords surgeons opportunities for trajectory modification based on real-time MRI to enhance procedural accuracy and safety of stereotaxis. We estimate the learning curve to involve 4 cases irrespective of the MRI suite used—after which ClearPoint-aided needle biopsies can be performed in time frames comparable with those reported for frame-based needle biopsy.

CRediT AUTHORSHIP CONTRIBUTION STATEMENT

Birra R. Taha: Data curation, Writing – original draft, Writing – review & editing, Visualization, Formal analysis. **Christian R. Osswald:** Data curation. **Matthew Rabon:** Data curation. **Carolina Sandoval Garcia:** Writing – review & editing. **Daniel J. Guillaume:** Writing – review & editing. **Xiao Wong:** Writing – original draft. **Andrew S. Venteicher:** Writing – review & editing. **David P. Darrow:** Writing – review & editing. **Michael C. Park:** Writing – review & editing. **Robert A. McGovern:** Methodology,

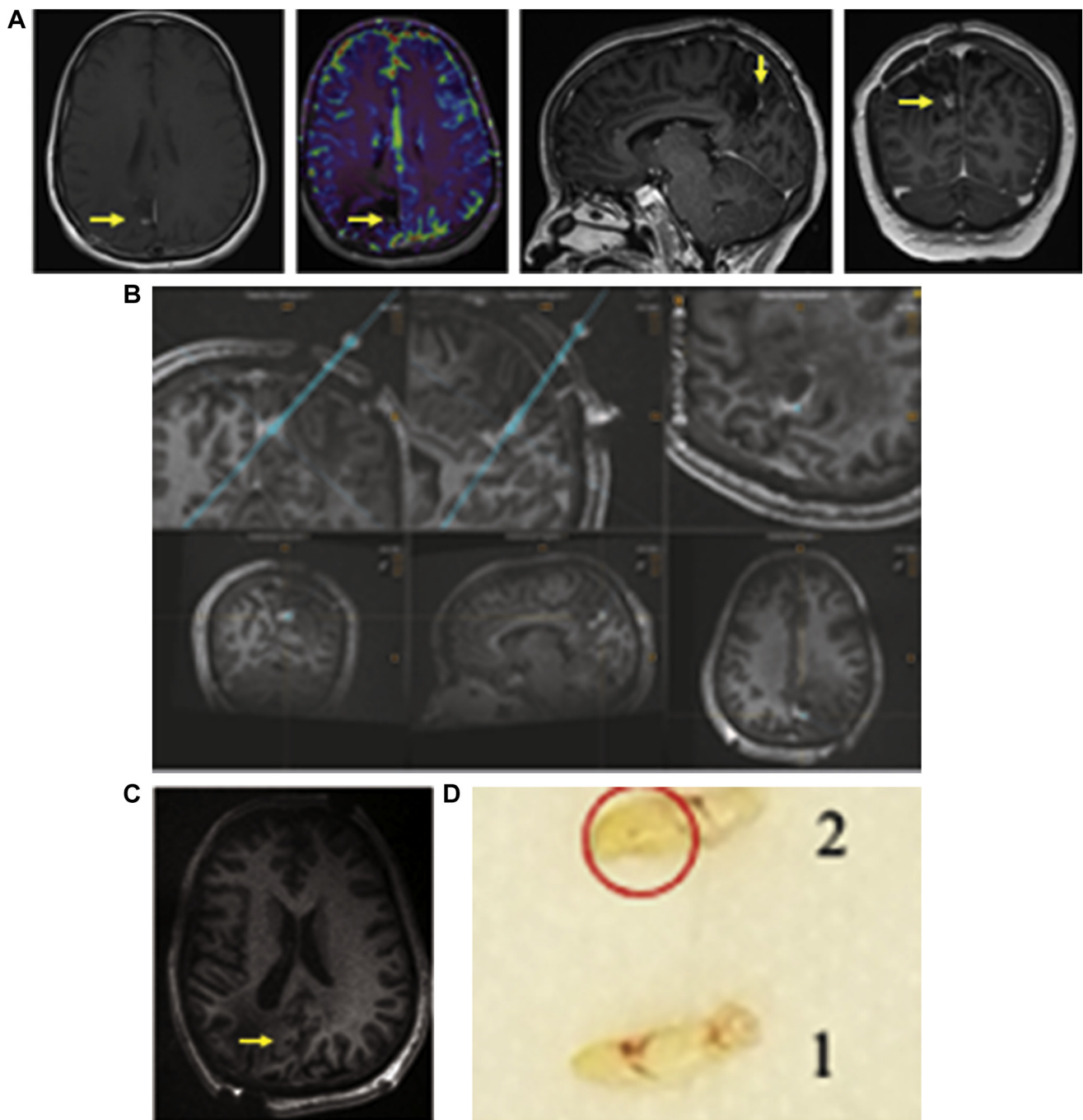


Figure 5. Sequential depth biopsy required for tissue diagnosis. **(A)** Axial, sagittal, and coronal magnetic resonance imaging (MRI) of a new contrast enhancing lesion in the posterior aspect of a previously resected grade III pleomorphic xanthoastrocytoma (PXA; IMRIS case 14). The region of contrast enhancement showed increased perfusion. **(B)** ClearPoint trajectory to the lesion. **(C)** Ceramic stylet was inserted to the confirm

biopsy site. **(D)** The initial biopsy showed the appearance of normal brain (labeled sample 1) and was nondiagnostic on frozen pathology. After a confirmatory MRI, the needle was advanced by 5 mm. Half of the biopsy taken at this site showed yellow discoloration (*red circle* on sample 2). Frozen pathology revealed recurrent PXA. The lesion was treated with laser interstitial thermotherapy after the biopsy.

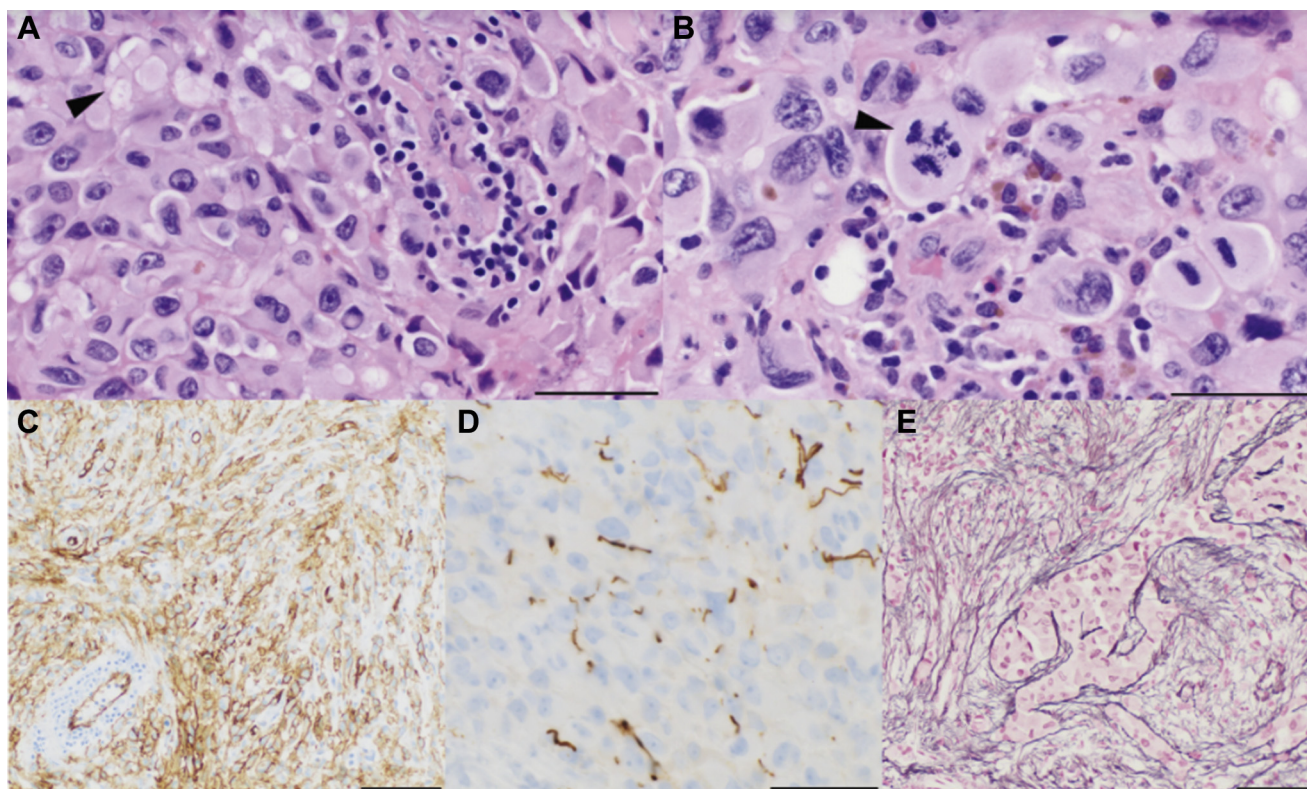


Figure 6. Anaplastic pleomorphic xanthoastrocytoma (PXA). **(A)** Lipidized astrocytes are observed (*arrowhead*). Perivascular lymphocytic cuffing (*right side*) within the neoplasm is a common feature (scale = 50 microns). **(B)** Bizarre, highly pleomorphic tumor cells with abundant cytoplasm is characteristic (scale = 50 microns). This case had increased mitotic activity (*arrowhead*), at least 5 mitoses per 10 high-power field and was designated

anaplastic PXA (scale = 100 microns). **(C)** CD34 expression was seen centrally within the neoplasm. **(D)** Neurofilament staining shows native axons are present peripherally and staining is negative centrally (not shown) consistent with mostly solid growth (scale = 50 microns). **(E)** Reticulin staining frequently demonstrates a patchy intercellular reticulin network or surrounding clusters of cells (scale = 100 microns).

Writing – review & editing. **Cornelius H. Lam:** Writing – review & editing. **Clark C. Chen:** Conceptualization, Methodology, Writing – review & editing, Supervision.

ACKNOWLEDGMENTS

We thank our operating room support staff as well as the MRI technologists for supporting these procedures.

REFERENCES

- Marcus HJ, Hughes-Hallett A, Kwasnicki RM, Darzi A, Yang G-Z, Nandi D. Technological innovation in neurosurgery: a quantitative study. *J Neurosurg.* 2015;123:174-181.
- Babu MA, Heary RF, Nahed BV. Device innovation in neurosurgery: controversy, learning, and future directions. *Neurosurgery.* 2012;70:789-794 [discussion: 794-795].
- Wilson CB. Adoption of new surgical technology. *BMJ.* 2006;332:112-114.
- Waters JD, Gonda DD, Reddy H, Kasper EM, Warnke PC, Chen CC. Diagnostic yield of stereotactic needle-biopsies of sub-cubic centimeter intracranial lesions. *Surg Neurol Int.* 2013;4(suppl 3):S176-S181.
- Bartek J Jr, Alattar A, Jensdottir M, Chen CC. Biopsy and ablation of H3K27 Glioma using skull-mounted SmartFrame device: technical case report. *World Neurosurg.* 2019;127:436-441.
- Scheer JK, Hamelin T, Chang L, Lemkuil B, Carter BS, Chen CC. Real-time magnetic resonance imaging-guided biopsy using SmartFrame® stereotaxis in the setting of a conventional diagnostic magnetic resonance imaging suite. *Oper Neurosurg (Hagerstown).* 2017;13:329-337.
- Carroll KT, Lochte BC, Chen JY, Snyder VS, Carter BS, Chen CC. Intraoperative magnetic resonance imaging-guided biopsy in the diagnosis of suprasellar Langerhans cell histiocytosis. *World Neurosurg.* 2018;112:6-13.
- Ivan ME, Yarlagadda J, Saxena AP, et al. Brain shift during bur hole-based procedures using interventional MRI. *J Neurosurg.* 2014;121:149-160.
- Alattar AA, Bartek J Jr, Chiang VL, et al. Stereotactic laser ablation as treatment of brain metastases recurring after stereotactic radiosurgery: a systematic literature review. *World Neurosurg.* 2019; 128:134-142.
- Chen C, Lee I, Tatsui C, Elder T, Sloan AE. Laser interstitial thermotherapy (LITT) for the treatment of tumors of the brain and spine: a brief review. *J Neurooncol.* 2021;151:429-442.
- Rennert RC, Carroll KT, Ali MA, et al. Safety of stereotactic laser ablations performed as treatment for glioblastomas in a conventional magnetic resonance imaging suite. *Neurosurg Focus.* 2016;41:E7.
- Ali MA, Carroll KT, Rennert RC, et al. Stereotactic laser ablation as treatment for brain metastases that recur after stereotactic radiosurgery: a multi institutional experience. *Neurosurg Focus.* 2016;41:E11.

13. Lang FF, Conrad C, Gomez-Manzano C, et al. Phase I study of DNX-2401 (Delta-24-RGD) oncolytic adenovirus: replication and immunotherapeutic effects in recurrent malignant glioma. *J Clin Oncol*. 2018;36:1419-1427.
14. R Core Team. R, version 3.3.2. Vienna, Austria: R Foundation for Statistical Computing; 2013.
15. Aiken R, Chen C, Cloughesy T, et al. ATIM-33. Interim results of a phase II multi-center study of oncolytic adenovirus DNX-2401 with pembrolizumab for recurrent glioblastoma; captive study (KEYNOTE-192). *Neuro Oncol*. 2019;21(suppl 6):vi8-vig.
16. Pan H, Cerviño LI, Pawlicki T, et al. Frameless, real-time, surface imaging-guided radiosurgery: clinical outcomes for brain metastases. *Neurosurgery*. 2012;71:844-851.
17. Stahl JE, Goldman JM, Rattner DW, Gazelle GS. Adapting to a new system of surgical technologies and perioperative processes among clinicians. *J Surg Res*. 2007;139:61-67.
18. Dhawan S, He Y, Bartek J Jr, Alattar AA, Chen CC. Comparison of frame-based versus frameless intracranial stereotactic biopsy: systematic review and meta-analysis. *World Neurosurg*. 2019;127:607-616.e4.
19. Mohyeldin A, Elder JB. Stereotactic biopsy platforms with intraoperative imaging guidance. *Neurosurg Clin N Am*. 2017;28:465-475.
20. Larson PS, Starr PA, Bates G, Tansey L, Richardson RM, Martin AJ. An optimized system for interventional magnetic resonance imaging-guided stereotactic surgery: preliminary evaluation of targeting accuracy. *Neurosurgery*. 2012;70(1 Suppl Operative):95-103. discussion 103.
21. Hamisch CA, Minartz J, Blau T, et al. Frame-based stereotactic biopsy of deep-seated and midline structures in 511 procedures: feasibility, risk profile, and diagnostic yield. *Acta Neurochir*. 2019;161:2065-2071.
22. Mohyeldin A, Lonser RR, Elder JB. Real-time magnetic resonance imaging-guided frameless stereotactic brain biopsy: technical note. *J Neurosurg*. 2016;124:1039-1046.
23. Hong CS, Beckta JM, Kundishora AJ, Elsamadicy AA, Chiang VL. Laser interstitial thermal therapy for treatment of cerebral radiation necrosis. *Int J Hyperthermia*. 2020;37:68-76.
24. Cheng G, Yu X, Zhao H, et al. Complications of stereotactic biopsy of lesions in the sellar region, pineal gland, and brainstem: a retrospective, single-center study. *Medicine (Baltimore)*. 2020;99:e18572.

Conflict of interest statement: C.C.C. serves as a consultant to ClearPoint Neuro. C.R.O. and M.R. are employees of ClearPoint Neuro, Inc.

Received 8 August 2021; accepted 26 November 2021

Citation: *World Neurosurg. X* (2022) 13:100115.
<https://doi.org/10.1016/j.wnsx.2021.100115>

Journal homepage: www.journals.elsevier.com/world-neurosurgery-x

Available online: www.sciencedirect.com

2590-1397/© 2021 The Author(s). Published by Elsevier Inc.
 This is an open access article under the CC BY-NC-ND license (<http://creativecommons.org/licenses/by-nc-nd/4.0/>).

